Predicting daily water table fluctuations in karstic aquifers from GIS-based modelling, climatic settings and extraction wells.

Concepcion Pla[a,b,*], Javier Valdes-Abellan[c], Antonio Jose Tenza-Abril[c], David Benavente[a,b]

[(a)] Departamento de Ciencias de la Tierra y del Medio Ambiente, Universidad de Alicante. Alicante, Spain.

[(b)] Laboratorio de Petrología Aplicada, Unidad Asociada UA-CSIC, Universidad de Alicante. Alicante, Spain.

[(c)] Departamento de Ingeniería Civil, Universidad de Alicante. Alicante, Spain.

*Corresponding Author: c.pla@ua.es

ABSTRACT

In semiarid regions, karstic aquifers are in some cases essential since they often constitute the only source of water supply. The increasing demand for water in these regions is responsible for the decreasing water table levels. As a consequence, groundwater management becomes indispensable. A robust black-box model of the Solana aquifer, a large karstic aquifer in Alicante province, is developed considering GIS-based modelling of the studied area, climatic settings and anthropic disturbances (water extractions and irrigation returns). The proposed model accurately predicts water table levels evolution (with EF index of 0.97 and RMSE of 0.09) and assesses the recharge rates. The model aims to become a useful tool in order to better understand the characteristics of karstic aquifers. A distinctive feature of the model is that it estimates the heterogeneous effective porosities along the depth profiles of the aquifer, which provides an advantage related to detect changes in the hydraulic transmissivity within karstic formations.

KEYWORDS

Karstic aquifer, recharge, effective porosity, semiarid regions, simple model.

1. Introduction

Estimating aquifer recharge is fundamental for determining water resources availability and assessing aquifer vulnerability to pollutants (Scanlon et al. 2002). Particularly, the groundwater is more heavily relied on to fulfill water demands due to its wide spread distribution and potable quality (Vashisht 2015). For sustainable management, water planners must know how much available water exists in the hydrological system to guarantee supply to all requirements (urban, agriculture, industry) with renewable abstraction, especially in the wake of increasing population and urban, industrial and agricultural demands (Abdulla 2009; Rejani et al. 2009). This fact is crucial in semiarid regions, well characterized by suffering a high degree of sensitivity to climate as consequence of highly variable rainfall, significantly lower than the evaporation rate (Mirzavand and Ghazavi 2014). Water resources systems have evolved in response to this variability, but in most regions of the world, rainfall variability continues to be a major source of uncertainty to address (Loukas et al. 2015).

Water management aims to solve the possible future problems related to water resources, which could be buffered by models and predictions of the fluctuations in groundwater levels (Emamgholizadeh et al. 2014). A proper management scheme allows the quantification of the recharge rate, which means the understanding of the hydrodynamic behaviour of the aquifer through a reliable characterization of the hydrogeological parameters (Sedki and Ouazar 2011; Sreekanth and Datta 2011; Werner et al. 2011; Chattopadhyay 2015).

The election of the most appropriate method to quantify the recharge becomes complicated (Scanlon et al. 2002). Complex models with many input parameters may produce more precise results but the uncertainties during the system characterization and the input data gathering process may lead to unreliable hydraulic property values.

Karstic aquifers, which constitute significant water reserves worldwide (El Janyani et al. 2014), are just a complex example of groundwater reservoirs characterized by the high heterogeneity of the carbonate system. Hydrologists have usually modelled karstic aquifers using distributed models (Harbaugh 2005; Schlumberger Water Services 2009) with homogeneous values (Scanlon et al. 2003; Martinez-Santos and Andreu 2010). However, the application of those models to karstic aquifers presents some controversial points due to (i) water flows in karstic aquifers are dominated by secondary (fracture) or tertiary (conduit) porosity; (ii) hierarchical permeability

structure or flow paths may exist, and (iii) turbulent flow component is likely to appear, which invalidates Darcy's law application used in most numerical models (Scanlon et al. 2003).

Alternative ways to confront that complexity consists of the use of lumped models, which consider aquifers as 'black or grey boxes' (Fleury et al. 2007) and whose use does not require detailed knowledge of physical hydrologic processes (Sang et al. 2015). These models are simpler but more robust and in many cases report results as good as more complex models (Martinez-Santos and Andreu 2010).

For instance, ERAS model (Aguilera and Murillo 2007, 2009) is one of the applied lumped models in SE Spain, a semiarid region where water sources from karstic aquifers account for most part of the total water demand. The model fits correctly to aquifers with deep water levels (as occur in many semiarid regions). In this model the evapotranspiration is calculated from temperature data, the model considers a geographically homogeneous infiltration process and assumes a uniform aquifer storage coefficient.

The main aim of this study is to develop a simple, trusty and robust black-box model to estimate water levels in karstic aquifers. Main characteristics of the presented model are the consideration of geographical heterogeneity in the different variables related to the aquifer surface (use of soil, surface slope, geology, precipitation, etc.) and the development of a routine to obtain non-uniform aquifer storage coefficients along the aquifer profile, which conforms the novelty of the proposed model. For this purpose, the model is applied to a 4-year period of piezometric data of Solana Aquifer.

2. Material and Methods

2.1. Study area

This modelling study focuses on Solana aquifer, a karstic aquifer with an extension of 268 km^2. Solana aquifer is located in the west sector of Alicante province (Fig. 1). The underground water reservoir is an essential source of water to the surrounding area (urban and agriculture), clearly influenced by the touristic industry. The mean measured annual precipitation on the aquifer area is nearly 350 mm and the average reference evapotranspiration (ET_0) is 1320 mm $year^{-1}$. Precipitation is the most important component of the aquifer recharge, while groundwater

abstraction is the only release. From fieldwork, we concluded that wells for water extraction are mainly located in the western area of the aquifer, to the left of the dry riverbank.

The main aquifer levels are formed by dolostone and limestone (Senonian – Turonian – Cenomanian ages) with a thickness of nearly 400 m and well developed karstification (Aragon-Rueda et al. 1992, 2003) which overlies a level of marls (Neocomian period) as the impervious layer. Aquifer limestone and dolostone materials outcrop in the northern area of the aquifer developing the Solana Mountain, an important recharge area of the aquifer (approximately 114 km^2) free of extraction wells.

Aquifer boundaries include three closed limits: an overthrusting of Solana complex above a synclinal folding (Fontanares synclinal) to the north; outcropping Keuper materials to the west and impermeable materials to the south. The eastern limit is settled by Mariola fault; some minimum water transfer was detected between Solana aquifer and the adjacent one through this limit (Aragon-Rueda et al. 2003) although the quantified transfer is not representative for recharge process.

Current demand in the region exceeds available natural supplies; the area has no permanent surface water bodies and the available water is obtained mostly from the aquifers exploitation. Pumped extraction from the Solana aquifer have exceeded natural recharge rates. In consequence, natural springs have disappeared throughout the last century (no active springs have been identified at this moment) and water table depth has dropped to more than 120 m depth.

2.2. Data collection

Required data used to calibrate the proposed model were obtained from various official sources. Water table depths were obtained from the Geological Survey of Spain, IGME, web page. Two monitoring wells were used to test our model: well 1 (W1, UTM: 697334, 4287040) and well 2 (W2, UTM: 694160, 4283750), identified with codes 2832-6-0010 and 2832-6-0019 respectively in the IGME inventory. These monitoring wells fully represent the water table levels trend in the valley comprised between Solana Mountain and the southern limit of the aquifer. There are other extraction wells in the study area, although information about the required parameters to calibrate the model is not easily accessible. Moreover, previous studies with a restricted amount of

monitoring points were successfully performed in areas with similar extensions (Long and Derickson 1999, Manglik and Rai 2000, Murillo et al. 2004, Nayak et al. 2006, Netzer et al. 2011).

Water extractions for the whole aquifer were obtained from Aguilera and Murillo (2007) and accounts for an average annual value of 35 hm^3 for the studied period (1994-1997). In addition, climatic settings (precipitation and temperature measurements) were obtained from AEMET (Meteorological National Agency of Spain) and were measured in three different meteorological stations located inside the aquifer boundaries (Fig. 1). Sample frequency is daily and ranges from 1994 to 1997 with no interruptions.

2.3. Modeling process

The complete modelling process has been divided into different stages in order to better understand its structure. Development of a Geographical Information System (GIS) document is the first step. Next, we establish the upper boundary conditions of the aquifer, in order to quantify water input and evapotranspiration. The third step bases on the calculation of the water balance; the final equation of our model allows obtaining water table fluctuations considering heterogeneous effective porosities along the aquifer depth profiles.

2.3.1. GIS-based modelling

The complete aquifer area was divided accordingly to the following categories (Fig. 2): (1) soil uses layer, containing 18 different classes; (2) soil slope layer with values classified as: <3%, 3-10%, 10-15%, 15-25% and >25%; (3) permeability qualitative distribution of the geological materials: high (dolostone and limestone materials), medium (quaternary gravels and sandy materials), low or very low permeability; and (4) weather stations site layer, which allows linking each location of the aquifer area with the most influential climatic station by the use of the Thiessen polygons method (Thiessen 1911). This process divided the study area in polygons, which were later clustered in 625 units by their same properties. GIS information was obtained from different public administrations: Valencian Cartographic Institute (ICV) and "Diputación Provincial de Alicante" (DPA). GIS process was carried out with Geomedia 6.1 ® software.

2.3.2. Upper boundary condition: evapotranspiration and water input

Reference evapotranspiration, $ET_{0\ i,j}$, was calculated daily for each polygon following the FAO Penman-Monteith method (Allen et al. 1998). The method is recommended as the sole standard

method for the definition and computation of the reference evapotranspiration and requires radiation, air temperature, air humidity and wind speed data. One of the advantages of using the FAO Penman-Monteith method is the fact that some of the data can be estimated with acceptable accuracy from other meteorological variables (Efthimiou et al. 2013). Reference evapotranspiration, $ET_{0\ i,j}$, is calculated as follows (Eq. 1):

$$ET_{0\ i,j} = \frac{0.408\Delta_{i,j}\left(R_{n\,i,j} - G_{i,j}\right) + \gamma_{i,j}\frac{900}{T_{i,j}+273}u_{2\ i,j}\left(e_{s\ i,j} - e_{a\ i,j}\right)}{\Delta_{i,j} + \gamma_{i,j}\left(1 + 0.34u_{2\ i,j}\right)} \quad (1)$$

where $ET_{0\ i,j}$ [mm day^{-1}]; $R_{n\ i,j}$ [MJ m^{-2}day^{-1}] is the net radiation at the crop surface; $G_{i,j}$ [MJ m^{-2}day^{-1}] is the soil heat flux density; $T_{i,j}$ [°C] is mean daily air temperature at 2 m height; $u_{2\ i,j}$ [m s^{-1}] is the wind speed at 2 m height; $e_{s\ i,j}$ [kPa] is the saturation vapour pressure; $e_{a\ i,j}$ [kPa] is the actual vapour pressure; $(e_{s\ i,j} - e_{a\ i,j})$ [kPa] is the saturation vapour pressure deficit; $\Delta_{i,j}$ [kPa °C^{-1}] is the slope vapour pressure curve; and $\gamma_{i,j}$ [kPa °C^{-1}] is the psychrometric constant. In our study, $G_{i,j}$ was assumed to be zero regarding that the time step was one day and the soil heat flux density is assumed to be relatively small compared to $R_{n\ i,j}$. For the studied period, the average annual precipitation and ET_0 were respectively 350 mm and 1320 mm, which is a conservable water loss value for the water balance. ET_0 is substantially higher during the summer when temperature is higher (mean summer temperature is 24.1 ^{0}C while mean winter temperature is 10.3 ^{0}C).

The runoff threshold values were obtained for each polygon of the aquifer area ($P0_i$), according to the Spanish normative (MOPU 1990). These coefficients are tabulated and essentially depend on the use, slope, hydrologic capacity and texture of soil. They are the equivalent of the SCS runoff curve numbers (Mockus 1954) but adapted to the local normative. The information is contained in the different GIS categories and associated to the different polygons where the $P0_i$ [mm] calculation is performed. The application of GIS to facilitate the estimation of runoff from ungauged catchments has gained increasing attention in recent years (Mdee 2015). As indicated in MOPU (1990), runoff coefficients, C_{ij}, [-] (i.e. a unitless proportion of the superficial component of the precipitation) were computed for each polygon of the aquifer area, *i*, and computational day, *j* (Eq. 2):

$$C_{i,j} = \frac{\left[\left(P_{i,j}/P0_i\right) - 1\right]\left[\left(P_{i,j}/P0_i\right) + 23\right]}{\left[\left(P_{i,j}/P0_i\right) + 11\right]^2} \quad (2)$$

where $P_{i,j}$ [mm] is the input precipitation data at polygon *i* and day *j*. If $P_{i,j}/P0_i < 1$, $C_{i,j} = 0$.

Input water on soil-aquifer system was calculated using Eq. 3.

$$IWnet_{i,j} = P_{i,j}(1 - C_{i,j}) \quad (3)$$

where $IWnet_{i,j}$ is the input water on soil aquifer [mm] at polygon *i* and day *j*; $P_{i,j}$ [mm] is the input precipitation data at polygon *i* and day *j*; and $C_{i,j}$ [-] is the runoff coefficient for the same polygon and day, previously defined.

2.3.3. Water balance computations

Soil-water balance and aquifer recharge are schematically described in Fig. 3. A soil water reservoir concept was established to model water flow through soil to the aquifer following the interesting approach that Fleury and others (Fleury et al. 2007) applied to the Fontaine de Vaucluse system. As they stated, soil was considered as a water reservoir. First, water input fills this reservoir and ET_0 acts uptaking the necessary water. Recharge to the aquifer is only produced if the soil reservoir is completely filled after ET_0 occurs. Eq. 4 summarizes the soil reservoir behaviour.

$$SR_{i,j} = SR_{i,j-1} + IWnet_{i,j} - ET_{0\,i,j} \quad (4)$$

where $SR_{i,j}$ [mm] is the soil reservoir value at polygon *i* and day *j;* and $SR_{i,j-1}$ [mm] is the soil reservoir at the same polygon the previous day. The rest of the terms have been defined previously. Eq. 5 summarizes the routine applied to quantify the water flow from the soil reservoir to the aquifer layer:

$$\text{if} \begin{cases} fc_i < SR_{i,j} & \rightarrow & \text{Re}_{i,j} = SR_{i,j} - fc_i \\ 0 < SR_{i,j} < fc_i & \rightarrow & \text{Re}_{i,j} = 0 \\ SR_{i,j} < 0 & \rightarrow & \text{Re}_{i,j} = 0 \qquad SR_{i,j} = 0 \end{cases} \quad (5)$$

where $Re_{i,j}$ [mm] is the recharge rate to the aquifer system at polygon *i* and day *j;* and fc_i [m^3 m^{-3}] is the field capacity at polygon *i*.

Fleury et al. (2007) considered that reservoir capacity is constant in the model. However, in our study we considered that the reservoir capacity varies for each polygon according to the field capacity of the soil. Values of soil capacity varied from 0.02 to 0.35 as proposed by (Twarakavi et al. 2009) and were assigned to the different polygons with GIS tools. Recharge is mainly accomplished through soils with low field capacity (like limestones outcrops) since soil reservoir is small and gets completely filled with low precipitation rates, rather than agricultural soils with high field capacity.

In our model, the next step was turning recharge length into total aquifer recharge volume by the consideration of the polygon areas. Calculation of recharge and soil reservoir volume was made for each polygon and then all of them were sum up along the aquifer area to obtain the total recharge in the aquifer (*Re*). Following this, once the aquifer total recharge volume was calculated, the model sums up the different direct water inputs and outputs to the total aquifer system (Fig. 3): (i) Total water extractions volume (*WE*). (ii) Values of irrigation returns (*IR*) to the aquifer system (0.85 hm^3 $year^{-1}$), which were obtained from previous studies (Rodriguez-Hernandez et al. 2010). (iii) Lateral inlets from neighbouring aquifer systems (*LI*). However, in our study lateral inlets can be set to zero since they are negligible (Aragon-Rueda et al. 1992). Computational time step was set up in one day and thus recharge rate and piezometric level variation were obtained for each day of the modelled period.

The Simplex search method of Lagarias et al. (1999) was applied to minimize the objective function value, defined as the sum of the square differences between the observed and modelled data by obtaining the best calibration factor values. In an initial iteration, all the factor values (f_1, f_2, f_3, f_4 and an initial effective porosity average value, p(z)) are calculated when comparing calculated piezometric level variations to real measured water table depths. The key of the proposed model is the use of different values of effective porosity (p(z)) along the depth of the profile, an inherent characteristic of the karstic aquifers. To considerer different values of effective porosity, the model estimates different p(z) depending on the input recharge volume and the resulted piezometric variation in the discretised depth profile. The model attributes differences between recharge volume and the resulting piezometric variation to changes in the effective porosity of the geologic material interfered by the water table as consequence of the karst development. The model recalculates the iteration by fitting the effective porosity (p(z) value) and obtains the definitive piezometric variations on each computational time step. Water extraction data and irrigation returns were not affected by any weighting factor since they were considered a credible value. All calculations of this stage were carried out using MATLAB R2011.a ® software.

Eq. 6 is the final implemented governing equation of the model.

$$\Delta z_j = \frac{f_1 \cdot Re_j - f_2 \cdot WE_j + f_3 \cdot IR_j + f_4 \cdot LI_j}{p(z) \cdot S_{aqf}} \qquad (6)$$

where Δz_j is the predicted water table fluctuation [m] at day *j*; Re_j [m³] is the recharge rate to the aquifer system at day *j*; WE_j [m³] is the water extraction from wells at day *j;* IR_j [m³] is the irrigation return data at day *j*; LI_j [m³] are the lateral inputs to the studied aquifer system, considered zero in the presented study; and S_{aqf} [m²] is the total aquifer surface; f_1 to f_4 are weighting factors [-]; and $p(z)$ is the effective porosity of the aquifer system [-]. Factor f_2 affecting water extraction from wells and f_3 affecting irrigation returns were set up to one following the abovementioned comment.

Eq. 6 shows that the presented model does not consider a unique value for effective porosity, as it is a general trend in other models, but it considers the triple porosity of the aquifer. Different types of elementary porosity components are commonly recognised in karst aquifers (Klimchouk 2006, and references cited hereby). Pores (primary porosity) are the pore space located between grains (intergranular porosity) and between crystals (intercrystalline porosity). Fissures (secondary porosity) are planar discontinuities such as bedding planes, joints and faults in which the aperture is negligible in scale when compared to the length and breadth. Tertiary porosity comes from secondary porosity modified by dissolution, that includes conduits, vugs and caverns. The proposed model considers the heterogeneity of the aquifer system, which is enhanced with the different obtained values of effective porosity. The idea becomes transcendent when dealing with karstic aquifers since groundwater accumulates mainly in the conduits, vugs and caverns rather than in the primary rock porosity.

2.3.4. Goodness of fit assessment

Obtained results were compared with observed values. For this purpose, we used graphical correlation and statistical indicators (Eqs. 7 and 8) based on the root mean square error (*RMSE*) and the Nash-Sutcliffe efficiency index (*EF*). The *EF* Index is a widely used statistic to assess the predictive power of hydrological models (Nash and Sutcliffe 1970).

$$RMSE = \frac{1}{x_{mean,o}} \sqrt{\frac{1}{n} \sum_{i=1}^{n} \left(x_{i,o} - x_{i,m}\right)^2} \tag{7}$$

$$EF = 1 - \frac{\sum_{i=1}^{n} \left(x_{i,o} - x_{i,m}\right)^2}{\sum_{i=1}^{n} \left(x_{i,o} - x_{mean,o}\right)^2} \tag{8}$$

where $x_{i,o}$ is the observed value at time *i*; $x_{i,m}$ is the predicted value at time *i*; and $x_{mean,o}$ is the mean observed value.

For *RMSE,* the optimal value is zero, indicative of a perfect fit between estimated and observed values, while threshold values of 0.2-0.3 are considered acceptable (Wallis et al. 2011). In the Nash-Sutcliffe Efficiency Index, $EF = 1$ for a perfect fit; $EF = 0$, when predicted values are as accurate as the mean of the observations; and $EF < 0$ indicates that model predictions are worse than the mean of observations. A threshold value of 0.68 was considered, following similar studies (Wallis et al. 2011).

2.3.5. Uncertainty assessment

In order to evaluate the uncertainty in the model parameters, its uniqueness and the uncertainty in water table predictions, the Generalized Likelihood Uncertainty Estimation, GLUE, method (Beven and Binley, 1992) was applied. The GLUE methodology is a Monte Carlo based technique, that allows a flexible definition of the likelihood function and its boundary value used to discriminate between behavioural and non-behavioural solutions. In this study we used the EF index, defined above, as the likelihood function following previous studies as the Beven and Binley (1992) or Mannina et al. (2010) with a threshold value of 0.1. More than 500.000 randomly chosen parameter sets were run and the performance of their respective model predictions was assessed by means of the likelihood measure. After rejection of the non-behavioural parameters sets, the weights of the behavioural sets were re-scaled. With the behavioural parameter sets, the predictive uncertainty bands associated with the 5% and the 95% were obtained.

3. Results and Discussion

GIS methodology classifies the material permeability as high and medium. Dolostone and limestone materials (high permeability) outcrop in the 44.6% of the area; and roads, industrial areas and urban equipment (very low permeability) compose the remaining 5.1% of the aquifer surface. Predominant soil slope (40% of the total surface) is in the range of 3-10%, but a substantial percentage of the area (26%) has slopes greater than 25%. Qualitative permeability classification reveals that more than 58% of the surface is composed by material with medium permeability whereas nearly 25% of the surface is classified as high permeability area. As a result, more than 80% of the surface presents appropriate properties to achieve aquifer recharge.

Experimental values and predictions of the water table depths for the studied wells (W1, W2) are shown in Fig. 4, which also illustrates precipitation, ET_0 and water extractions for the studied

period. Water table depths followed a nearly constant decreasing tendency for this period accounting a total water table decrease of 32 and 28 m for W1 and W2 respectively. This decrease was accentuated from March 1995 to August 1996, by the severe lack of water during summer 1994 and summer 1996. In addition, summer periods are characterized by important increases in water extractions from the Solana aquifer, which exceeded 35 hm^3 $year^{-1}$ for irrigation, as well as increases in ET_0 values. Some smooth recoveries of the water table depths are identified for the whole period but they did not last long; the most remarkable was found after the important precipitation event in March 1995 (295.6 mm).

Figure 4 reveals that experimental water table depths were accurately predicted by the model for both wells. Mean differences between experimental and predicted values of water table depth are 1.4 and 1.3 m for wells W1 and W2 respectively. Highest differences are found in February 1994 and June 1995 for well W1; and June 1994 and September 1994 for well W2. Nevertheless, the general trend in both wells was properly captured, which confirms that the proposed model achieves accurate values of water table depth variations in Solana aquifer. The model proposed by Murillo et al. (2004) performed in the Solana aquifer, was also accurate although differences between experimental and predicted values were nearly 10 m in some cases. In addition, no consideration of the effective porosity differences was taking into account.

In the proposed model, predicted values showed a quick response to changes in the prevailing climatic conditions following the same trend of the experimental data, both in periods with no precipitation (summers of 1994 and 1996) and in periods with very intense rainfalls. These predictions for both wells may validate the inclusion of the soil reservoir water concept in the proposed model, as it was established in previous studies (Fleury et al. 2007).

Estimated porosity profiles for both studied wells W1 and W2 (Fig. 5) reveal that mean effective porosity values are 0.008 and 0.013 respectively. Porosity values in the aquifer are variable and depend on the tertiary fraction. Pore volume in the limestones is low (less than 0.05), which is in accordance with our results. Relationship between calculated porosity values and the principal geological materials (dolostones and limestones) confirms that the application of the model fits well to karstic aquifers.

The contribution of fissures to porosity may be considered to be negligible, although they are essential to water flows (Dullien 1992). Tertiary porosity in the aquifer presents a dual character

with regard to water flow and storage. In well W1, maximum values of effective porosity appear at 410 m.a.s.l. (≈0.011) and a very low effective porosity region appears at 392 m.a.s.l. After that region, effective porosity increases its value (≈0.008), which seems to keep nearly constant up to the end of the profile. In well W2, a similar pattern is described, with the lowest values of effective porosity (≈0.0009) around 384 m.a.s.l. These similar very low effective porosity regions could be related with the same geological formation in both wells. Nevertheless, at the end of the profile in W2, significant increases of effective porosity (≈0.019) are found, which point to the presence of a well-developed karstification around 400-410 m.a.s.l., probably related with calcite dissolution and karstic structures formation. Wells W1 and W2 are located in the same region of the aquifer area and, therefore, approximately the same domains in the both wells profiles would be expected.

The effective porosity values allow obtaining a precise equation to estimate the water table depth variations (Eq. 6). Table 1 shows the results for factors f_1 to f_4 for both studied wells. Slight differences appear between factors for the two wells, highlighting the existing spatial heterogeneity between the two well locations, even considering that both wells are located in the same domain. This fact supports the idea of not using homogeneous models in karstic aquifers.

Results are indicative of the system response as highlighted by EF index and RMSE values. EF results were 0.97 for both wells. In addition, satisfactory results were found when calculating the RMSE between the calculated and measured values. Results of RMSE were 0.09 for both wells. These results confirmed that the model gave a reliable simulation of the aquifer´s temporal evolution.

The uncertainty of parameters and results was calculated. Figure 6 shows the changes in the RMSE index related to variations in the input variable (f_1, f_2 and p(z)) in W1 and W2. Results demonstrate that f_1 (affecting to the recharge rate of the aquifer) is the most sensible parameter in the proposed model.

In addition, the predicted values (piezometric levels) were located between the two uncertainty bands (5% and 95% percentiles). Figure 4 also shows that the uncertainty of the water table predictions increases along time, which is a consequence of the model structure that computes water table variations each day and sums all previous values.

Through this proposed method, variations of the effective porosity in the depth profile are evaluated. The lithologic heterogeneity, which affects permeability and other hydraulic parameters

in the aquifer, can provide quantitative data for use in fluid-flow modeling (Cunningham 2004) and to identify the internal organization of lithologic units.

Considering future work, the application of the recent findings to karstic systems will allow evaluating the proposed model in a high range of aquifers. In addition, we consider that the application of this methodology to several wells of the aquifer area would allow obtaining a 3-D characterisation of the karstic aquifer features.

4. Conclusions

Estimating aquifer recharge is fundamental in areas where water scarcity constrains the potential development of the society. This study presents a geographical distributed black-box model tool to assess aquifer recharge and water table evolution in karstic aquifers.

This model requires GIS-based modelling of the studied area and climatic characterization but does not require precise characterization of the aquifer domain and its boundaries, which constitutes an important advantage. Among the required inputs for the model, water extractions from the aquifer were the most difficult data to obtain, since water managers are reluctant to give this information, even more so in arid regions where there is not enough water for all demanders and potential users.

Results showed that the model is able to accurately predict the evolution of the water table in both wells for four complete hydrological years. The model is based on the inclusion of weighting parameters and it allows detecting the spatial heterogeneities along the aquifer profile. For this reason, the model has proved to be useful in karstic mediums, where effective porosity may vary along the depth of the aquifer where the piezometric level ranges. The adjustment of the presented model to wells in Solana aquifer confirmed the changes in the effective porosity in the depth profile, an inherent characteristic of the karstic aquifers.

This feature gives an important advantage in case of karstic aquifers, where groundwater location is fully dependent of the presence of well-developed cavities. In addition, using heterogeneous values of porosity along the depth of the aquifer reports a more realistic approach to the reality of karstic aquifers; and by comparison of the depth profiles from different wells, hydrologists are able to better understand and identify the aquifer structure.

Acknowledgements

This study was partially financed by the Spanish Ministry of Economy and Competitiveness Project CGL2011-25162. A pre-doctoral research fellowship (BES-2012-053468) was awarded to C. Pla for this project. The authors are extremely grateful to Dr. Jose Miguel Andreu for his helpful comments and suggestions about the ground water hidrology.

Conflict of interest

No conflict of interest.

References

Abdulla F, Eshtawi T, Assaf H (2009) Assessment of the impact of potential climate change on the water balance of a semi-arid watershed. Water resour manag 23(10):2051-2068. doi: 10.1007/s11269-008-9369-y

Aguilera H, Murillo JM (2007) Application of the "ERAS" model to estimate aquifer recharge time series and their relation to climate change in four karstic aquifers from the High Vinalopo County (Alicante). Aplicación del modelo "ERAS" a la elaboración de series históricas de recarga natural y su relación con el cambio climático en cuatro acuíferos kársticos de la comarca del Alto Vinalopó (Alicante). Boletín Geológico y Minero 118 (1):63-80.

Aguilera H, Murillo JM (2009) The effect of possible climate change on natural groundwater recharge based on a simple model: A study of four karstic aquifers in SE Spain. Environ Geol 57(5):963-974.

Allen RG, Pereira LS, Raes D, Martin S (1998) Crop evapotranspiration - Guidelines for computing crop water requirements - FAO Irrigation and drainage paper 56. FAO, Rome.

Aragon-Rueda R, Rodriguez-Hernandez L, Barba-Romero J (1992) Evaluacion de los recursos hidricos subterraneos y propuesta de normas de explotacion de la unidad de Solana. IGME. IGME web. http://info.igme.es/ConsultaSID/presentacion.asp?Id=67091. Accessed 22 February 2014.

Aragon-Rueda R, Solis L, Gambín J, Quintana JL (2003) Determinación de las reservas útiles en acuíferos de abastecimiento público en Alicante: acuíferos Solana, Maigmó, Sella, Beniardá-Polop y Solana de la Llosa. IGME-DPA. IGME web. http://info.igme.es/ConsultaSID/presentacion.asp?Id=80505. Accessed 22 February 2014.

Beven K and Binley A (1992) The future of distributed models: model calibration and uncertainty prediction. Hydrol Processes 6: 279-298. doi: 10.1002/hyp.3360060305

Chattopadhyay PB, Vedanti N, Singh VS (2015) A Conceptual Numerical Model to Simulate Aquifer Parameters. Water Resour Manag 29(3):771-784. doi:10.1007/s11269-014-0841-6

Cunningham KJ (2004) Application of ground-penetrating radar, digital optical borehole images, and cores for characterization of porosity hydraulic conductivity and paleokarst in the Biscayne aquifer, southeastern Florida, USA. J Appl Geophys 55(1–2):61-76. doi:10.1016/j.jappgeo.2003.06.005.

Dullien FAL (1992) Porous Media Fluid Transport and Pore Structure. Academic Press, San Diego.

Efthimiou N, Alexandris S, Karavitis C, Mamassis N (2015) Comparative analysis of reference evapotranspiration estimation between various methods and the FAO56 Penman - Monteith procedure. Eur Water 42:19-34, 2013

El Janyani S, Dupont JP, Massei N, Slimani S, Dörfliger N (2014) Hydrological role of karst in the Chalk aquifer of Upper Normandy, France. Hydrogeol J 22(3):663-677. doi: 10.1007/s10040-013-1083-z

Emamgholizadeh S, Moslemi K, Karami G (2014) Prediction the groundwater level of bastam plain (Iran) by artificial neural network (ANN) and adaptive neuro-fuzzy inference system (ANFIS). Water Resour Manage 28(15):5433-5446. doi:10.1007/s11269-014-0810-0

Fleury P, Plagnes V, Bakalowicz M (2007) Modelling of the functioning of karst aquifers with a reservoir model: Application to Fontaine de Vaucluse (South of France). J Hydrol 345(1-2):38-49. doi:10.1016/j.jhydrol.2007.07.014

Harbaugh AW (2005) MODFLOW-2005:The U.S. Geological Survey Modular Ground-Water Model. The Ground-Water Flow Process. U.S. Geological Survey Techniques and Methods 6–A16. Reston, Virginia, USA.

Klimchouk, A (2006) Unconfined Versus Confined Speleogenetic Settings: Variations of Solution Porosity. Int J Speleol 35(1):19-24.

Lagarias JC, Reeds JA, Wright MH, Wright PE (1999) Convergence properties of the Nelder-Mead simplex method in low dimensions. SIAM J Optim 9(1):112-147.

Long AJ, Derickson RG (1999) Linear systems analysis in a karst aquifer. J Hydrol 219(3-4): 206-217. doi: 10.1016/s0022-1694(99)00058-x

Loukas A, Sidiropoulos P, Mylopoulos N, Vasiliades L, Zagoriti K (2015) Assessment of the effect of climate variability and change and human intervention in the lake Karla aquifer. Eur Water 49:19-31.

Manglik A, Rai SN (2000) Modeling of Water Table Fluctuations in Response to Time-varying Recharge and Withdrawal. Water Resour Manage 14(5):339-347. doi: 10.1023/a:1011154903100

Mannina G, Di Bella G, Viviani G (2010) Uncertainty assessment of a membrane bioreactor model using the GLUE methodology. Biochem Eng J 52(2-3): 263-275. doi:10.1016/j.bej.2010.09.0

Martinez-Santos P, Andreu JM (2010) Lumped and distributed approaches to model natural recharge in semiarid karst aquifers. J Hydrol 388(3-4):389-398. doi:10.1016/j.jhydrol.2010.05.018

Mdee OJ (2015) Spatial distribution of runoff in ungauged catchments in Tanzania. Water Util J 9:61-70.

Mirzavand M, Ghazavi R (2015) Stochastic Modelling Technique for Groundwater Level Forecasting in an Arid Environment Using Time Series Methods. Water Resour Manage 29(4):1315–1328. 10.1007/s11269-014-0875-9

Mockus V (1954) Hydrology Guide for Use in Watershed Planning. Soil Conservation Service. United States.

MOPU (1990) Norma 5.2-IC - Drenaje superficial. Instrucción de carreteras. España.

Murillo JM, De la Orden JA, Roncero FJ (2004) El modelo ERAS. una herramienta sencilla para estimar la recarga a los acuíferos que tienen una respuesta rápida. Congreso XXXIII IAH 7º - ALHSUD. Groundwater flow understanding: for local to regional scales. Zacatecas City, Méjico.

Nash JE, Sutcliffe JV (1970) River flow forecasting through conceptual models part I — A discussion of principles. J Hydrol 10(3):282-290. doi:10.1016/0022-1694(70)90255-6

Nayak PC, Satyaji Rao YR, Sudheer KP (2006) Groundwater Level Forecasting in a Shallow Aquifer Using Artificial Neural Network Approach. Water Resour Manage 20(1):77-90. doi: 10.1007/s11269-006-4007-z

Netzer L, Weisbrod N, Kurtzman D, Nasser A, Graber ER, Ronen D (2010) Observations on Vertical Variability in Groundwater Quality: Implications for Aquifer Management. Water Resour Manage 25(5):1315-1324. doi: 10.1007/s11269-010-9746-1

Rejani R, Jha MK, Panda SN (2009) Simulation-optimization modelling for sustainable groundwater management in a coastal basin of Orissa, India. Water resour manage 23(2):235-263. doi: 10.1007/s11269-008-9273-5

Rodriguez-Hernandez L, Fernandez-Mejuto M, Hernandez-Bravo JA (2010) Mapa Hidrogeológico. Provincia de Alicante. Diputación Provincial de Alicante. Alicante.

Sang YF, Wang Z, Liu C (2015) Wavelet Neural Modeling for Hydrologic Time Series Forecasting with Uncertainty Evaluation. Water Resour Manage. doi: 10.1007/s11269-014-0911-9

Scanlon BR, Healy RW, Cook PG (2002) Choosing appropriate techniques for quantifying groundwater recharge. Hydrogeol J 10(1):18-39. doi:10.1007/s10040-001-0176-2

Scanlon BR, Mace RE, Barrett ME, Smith B (2003) Can we simulate regional groundwater flow in a karst system using equivalent porous media models? Case study, Barton Springs Edwards aquifer, USA. J Hydrol 276(1-4):137-158. doi:10.1016/S0022-1694(03)00064-7

Schlumberger Water Services (2009) Visual MODFLOW 2009.1. User's Manual. Schlumberger Water Services. Waterloo, Ontario, Canada.

Sedki A, Ouazar D (2011) Simulation-optimization modeling for sustainable groundwater development: a Moroccan coastal aquifer case study. Water Resour Manage 25(11):2855–2875. doi: 10.1007/s11269-011-9843-9

Sreekanth J, Datta B (2011) Comparative evaluation of genetic programming and neural network as potential surrogate models for coastal aquifer management. Water Resour Manage 25(13):3201–3218. doi: 10.1007/s11269-011-9852-8

Thiessen AH (1911) Precipitation averages for large areas. Mon Wea Rev 39(7):1082-1089. doi: 10.1175/1520-0493(1911)39<1082b:PAFLA>2.0.CO;2

Twarakavi NKC, Šimůnek J, Schaap MG (2009) Development of Pedotransfer Functions for Estimation of Soil Hydraulic Parameters using Support Vector Machines. Soil Sci Soc Am J 73(5):1443-1452. doi: 10.2136/sssaj2008.0021

Vashisht AK (2015) Adaption of seepage spring development technique to manage the water scarcity in Himalayan region – A practical approach. Water Util J 11:93-98.

Wallis KJ, Candela L, Mateos RM, Tamoh K (2011) Simulation of nitrate leaching under potato crops in a Mediterranean area. Influence of frost prevention irrigation on nitrogen transport. Agr Water Manage 98(10):1629-1640. doi:10.1016/j.agwat.2011.06.001

Werner A, Alcoe D, Ordens C, Hutson J, Ward J, Simmons C (2011) Current practice and future challenges in coastal aquifer management: flux-based and trigger-level approaches with application to an Australian case study. Water Resour Manage 25(7):1831–1853. doi: 10.1007/s11269-011-9777-2

Tables

Table 1 Values of calibration factors for wells W1 and W2.

	f_1	f_2	f_3	f_4
Well 1	0.351	1	1	0
Well 2	0.2241	1	1	0

Figures

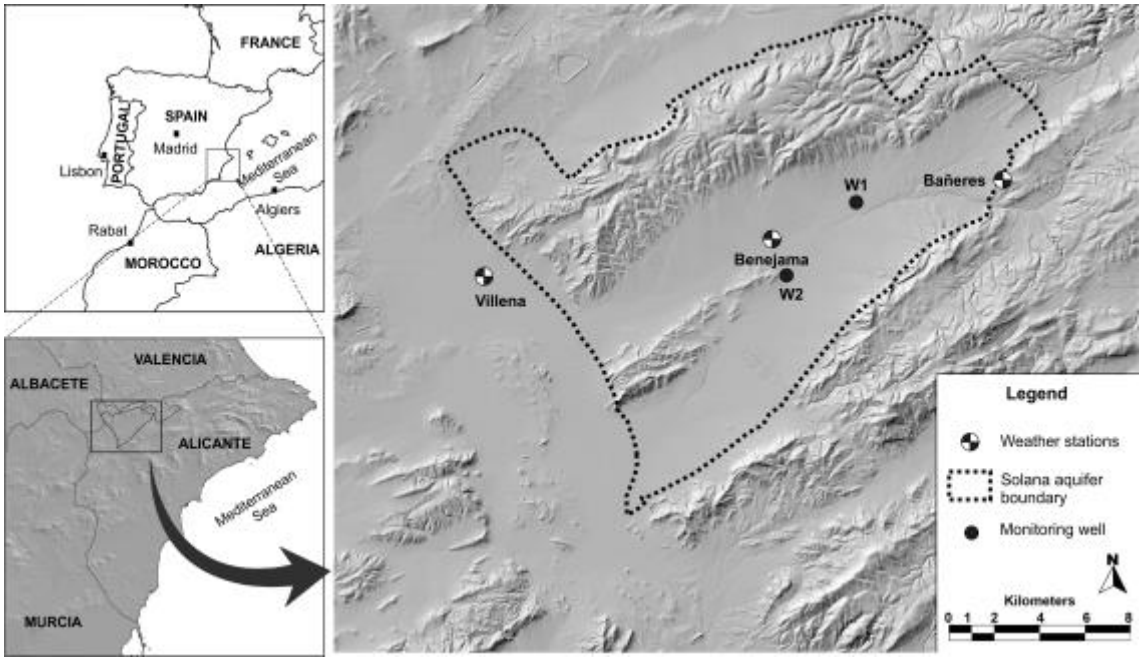

Fig. 1 Study area and location of the Solana aquifer.

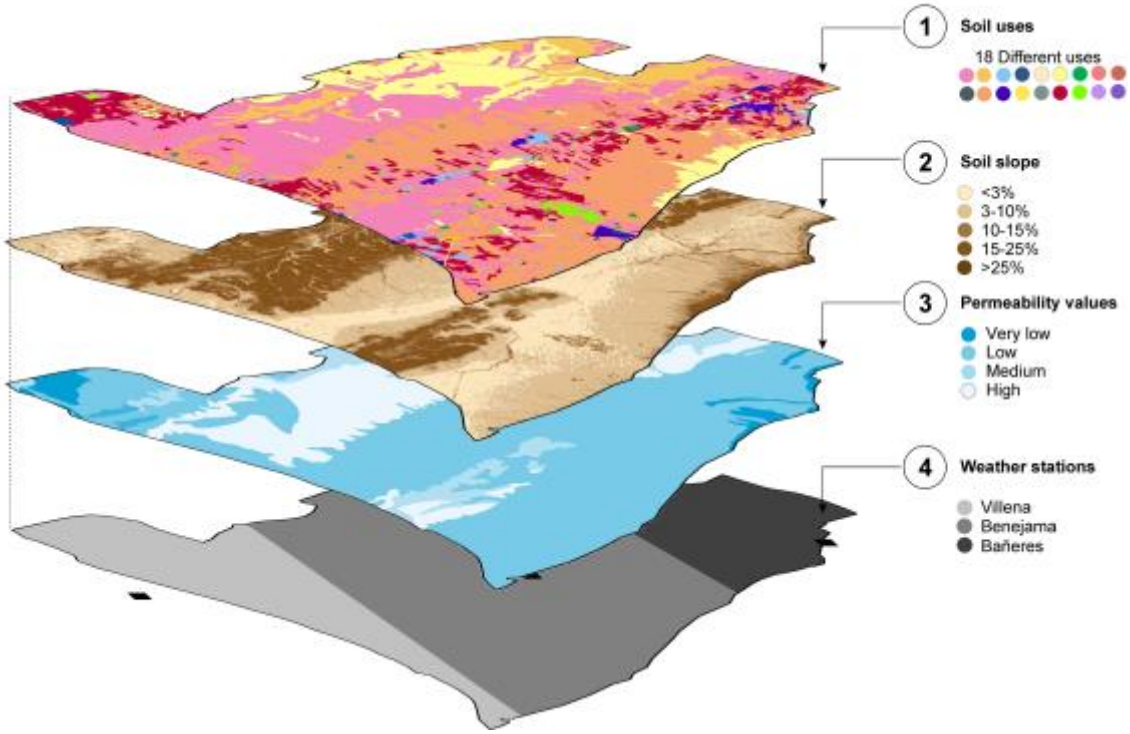

Fig. 2 GIS layers and subclasses classification.

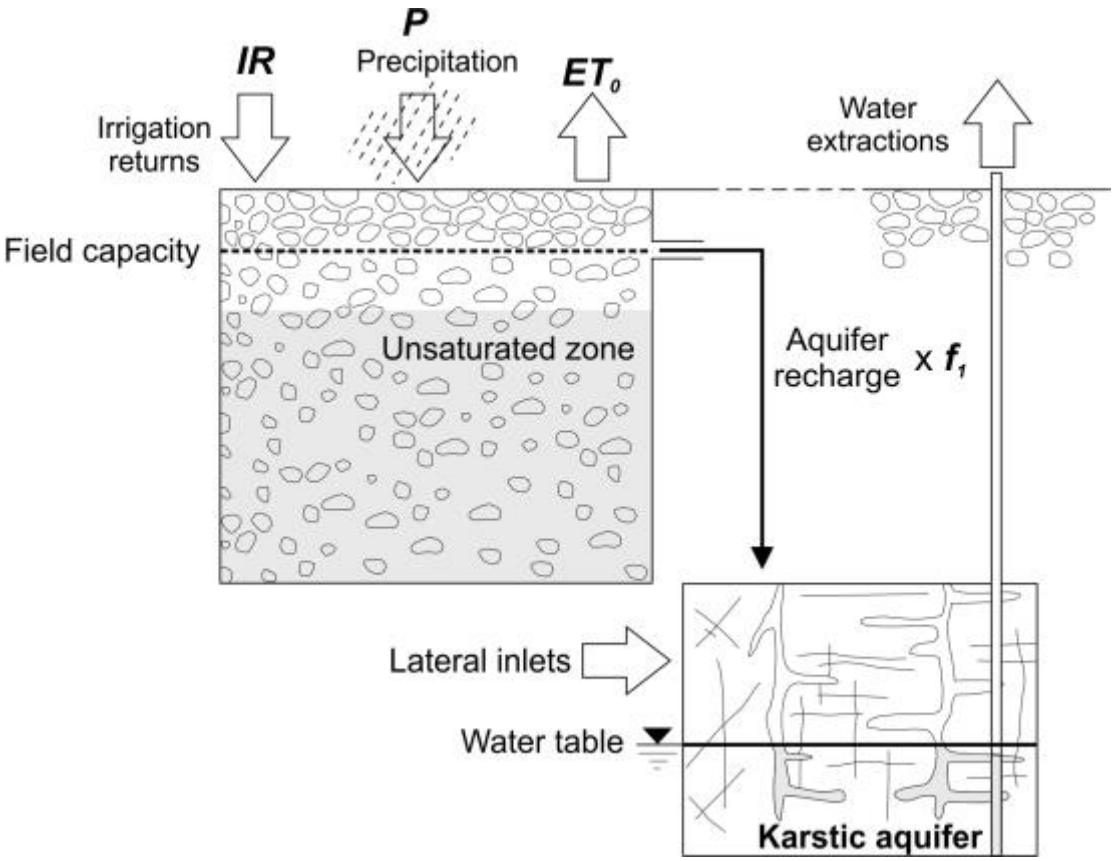

Fig. 3 Scheme of the proposed water balance model in the soil.

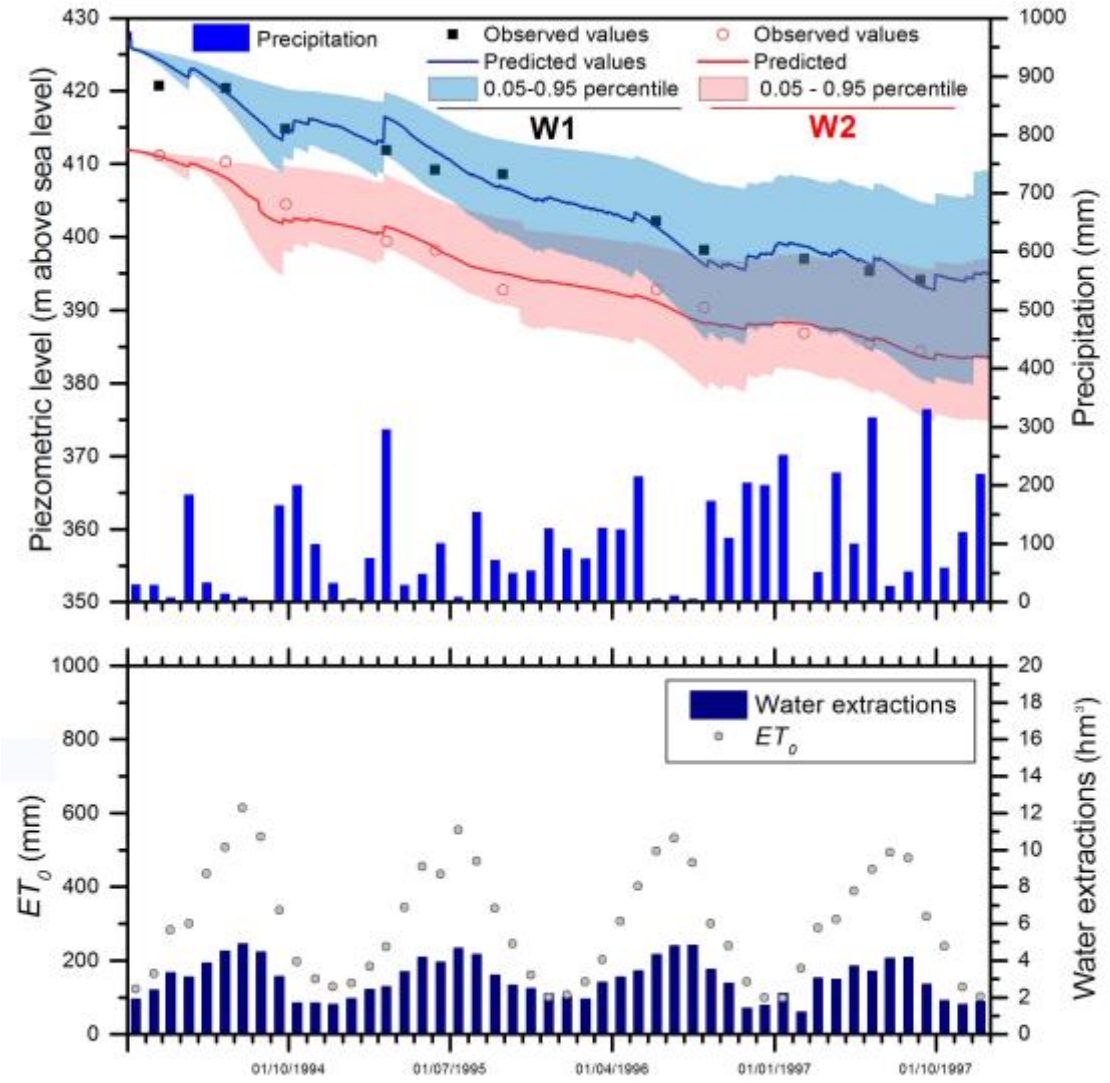

Fig. 4 Predicted and observed data in wells W1 and W2. Water extractions and climatic settings (precipitation and ET_0). Predictive uncertainty bands associated with the 5% and the 95% percentiles obtained for the model.

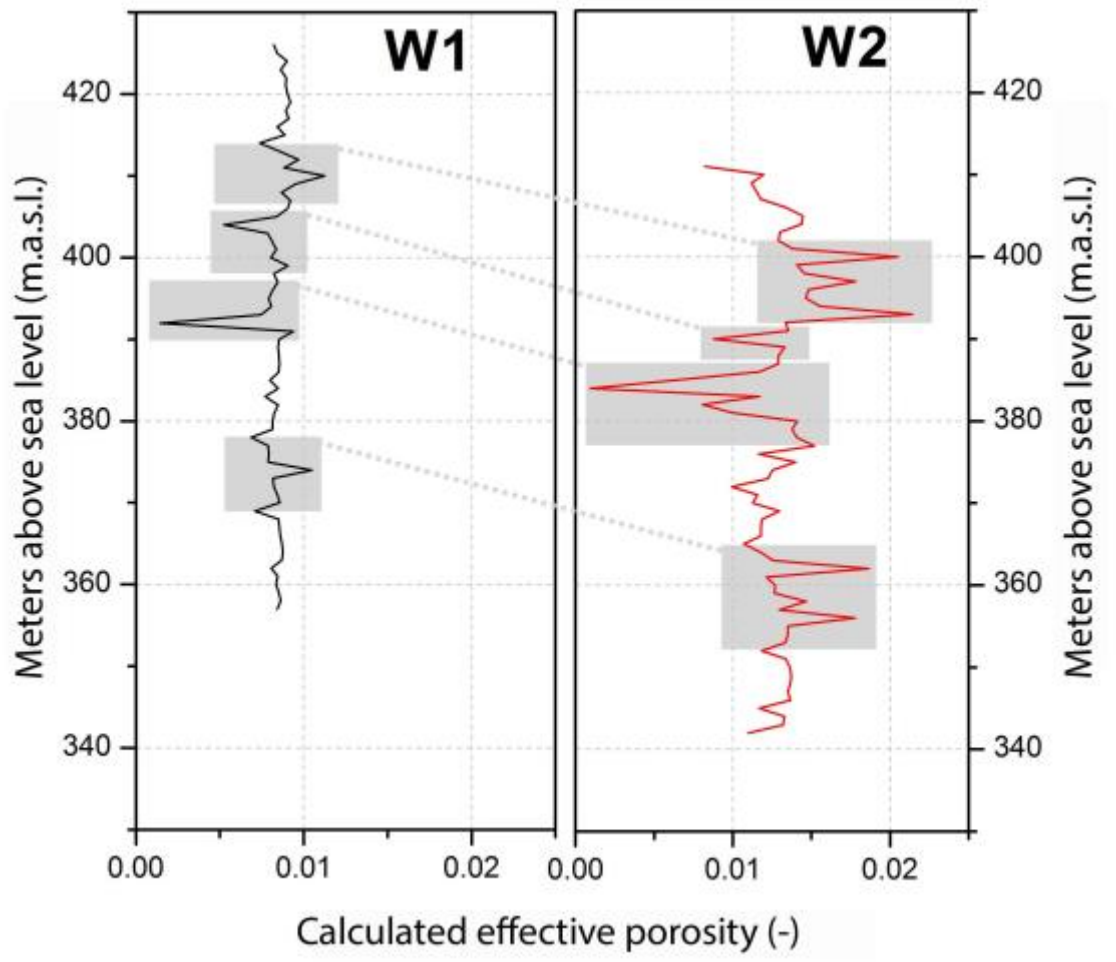

Fig. 5 Calculated effective porosity profiles for wells W1 and W2.

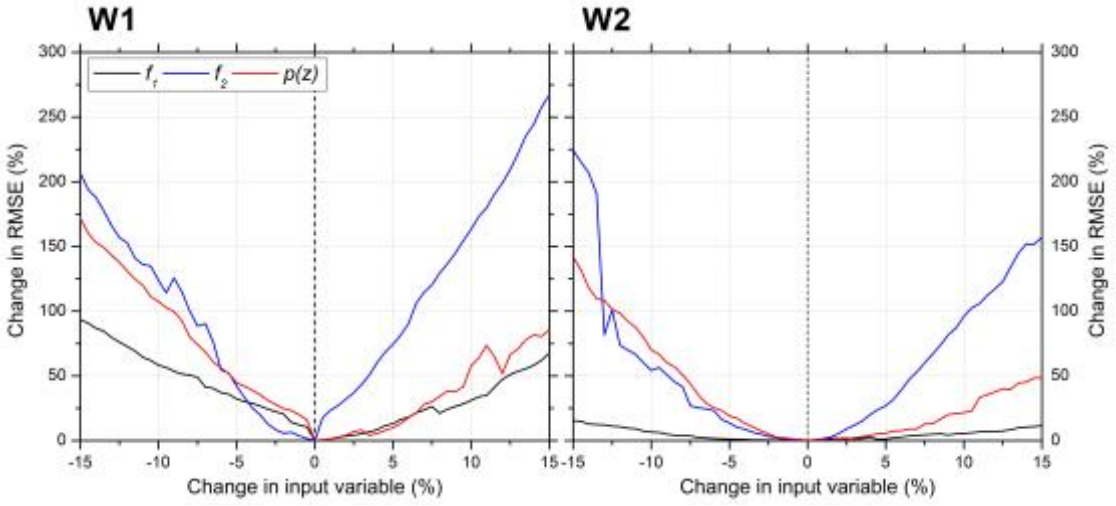

Fig. 6 Changes in the RMSE index related to variations in the input variable (f_1, f_2 and p(z)) in W1 and W2.